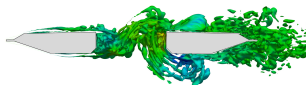
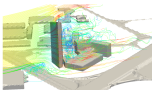


Numerical simulation of a 5:1 rectangular cylinder at non-null attack angles

Mattia Ricci¹ Luca Patruno¹

¹University of Bologna, Laboratory of Computational Mechanics

HPC enabling OpenFOAM for CFD applications, 2015



Outline

1

Introduction

2

Computational model

- Computational Domain
- Mesh
- Numerical setup for LES
- Numerical setup for RANS
- HPC facility

3

Numerical Results

- Convergence
- Flow Topology and Bulk Parameters
- Central Section Statistics
- Spanwise Averaged Statistics and Correlations
- Covariance Proper Transformation

4

Summary

- Conclusions
- Unipol Tower and Decks

CFD for Civil Engineering Applications

Computational Fluid Dynamics is becoming an increasingly attractive tool for the investigation of the flow field around structures relevant for civil engineering applications.

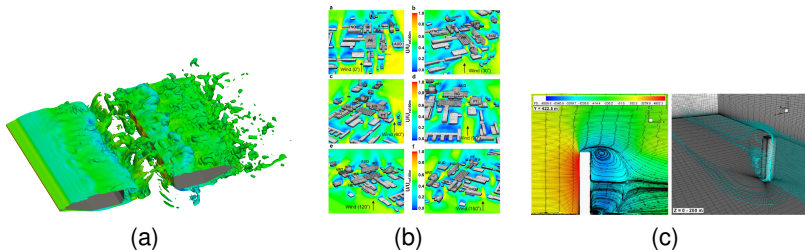


Figure: Aerodynamic study of bridge decks [1] (a), Aeroelastic analysis of tall buildings [2] (b), Pedestrian wind comfort around buildings [3] (c).

Simulations results are very scattered!

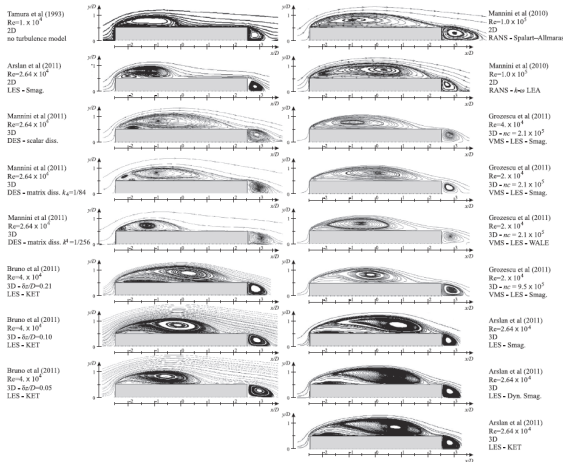
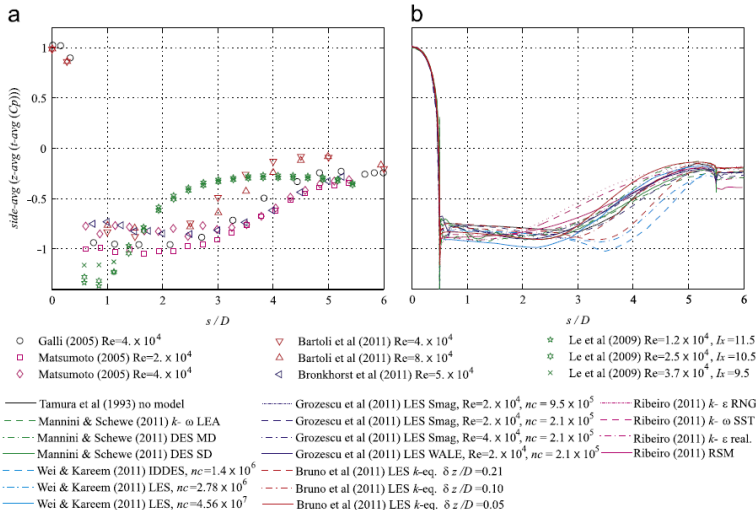


Fig. 7. Time and spanwise-averaged streamlines.

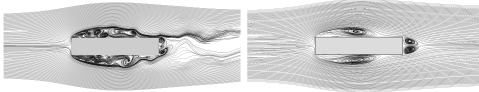
- The capability of such techniques in reproducing the complex flow fields observed around bluff bodies at high Re , is still a very active research topic.
- Even for what concerns simple geometries the accurate simulation of turbulent flows represents a challenging engineering problem.

Experimental data are very scattered!

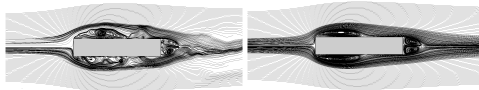


Turbulence model and Numerical Schemes effects

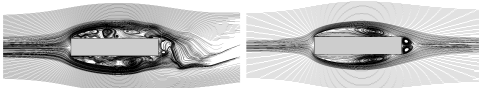
Static Smag. LUST 5M



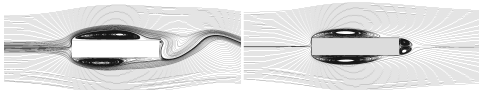
Dynamic Smag. LUST 5M



Static Smag. Upwind 13M

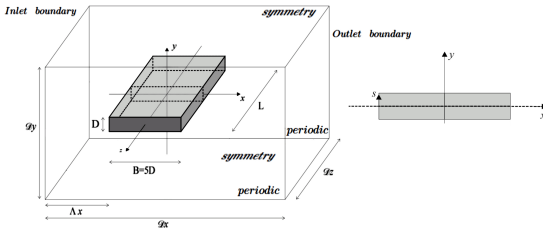


RANS

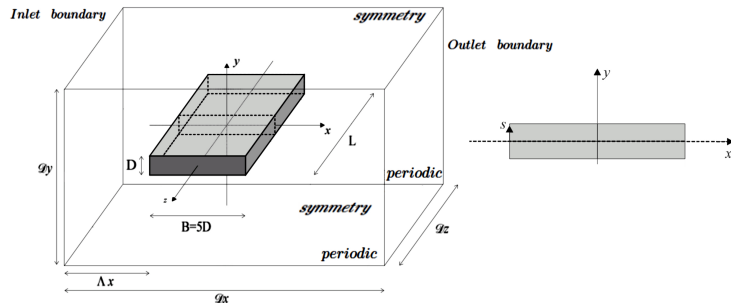


Problem Statement

- The smooth flow around a rectangular cylinder 5:1 at $Re = 2.7 \times 10^4$ is studied by using LES and RANS approaches.
- 3 different attack angles are considered, namely: 0, 1, 4 degrees.
- Results in terms of pressure distributions are compared with experimental data available.

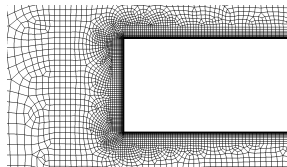
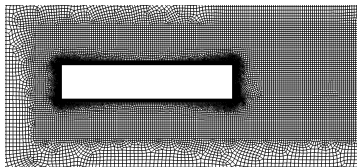


Computational Domain

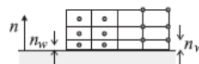
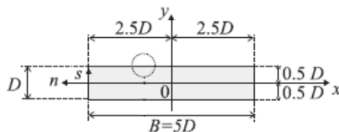


Source	Dim	D_x/B	D_y/B	D_z/B	Λ_x/B
LES	3D	40	30	2	16
RANS	2D	40	30	—	15
Bruno et al. (2010, 2011)	3D	41	30.2	1, 2, 4	15
Grozescu (2011)	3D	41	30.2	1	15
Mannini (2011)	3D	200	200	1, 2	100

Mesh Section



Source	n_w/B	δ_x/B	δ_z/B
LES	5.0×10^{-4}	2.5×10^{-3}	0.02
RANS	5.0×10^{-4}	2.5×10^{-3}	—
Bruno et al. (2010, 2011)	5.0×10^{-4}	2.0×10^{-3}	0.042 – 0.01
Grozescu (2011)	$5 \times 10^{-4}, 2.5 \times 10^{-4}$	$1.0 \times 10^{-2}, 5 \times 10^{-3}$	0.042, 0.01
Mannini (2011)	5.0×10^{-5}	1.4×10^{-2}	0.0156



Mesh adopted for LES

The LES is performed in a 3D framework.

- the mesh is extruded along z direction for a total length $D_z = 2.0B$;
- the cell size in the extrusion direction is equal to $\delta_z/B = 0.02$;
- the resultant mesh counts about $5.5M$ of finite volumes ;
- the computational domain is larger enough to avoid blockage ratio (0.6%) effects ;
- the distance of the body from the faces of the domain is considered sufficient to avoid boundary conditions effects.

Mesh adopted for LES

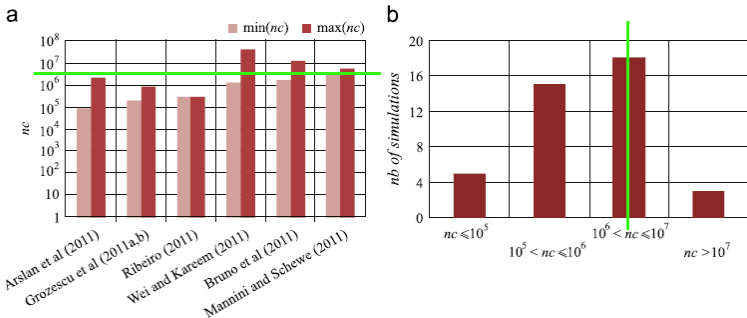


Figure: Comparisons with other simulations [4].

Numerical setup for LES

Boundary Conditions

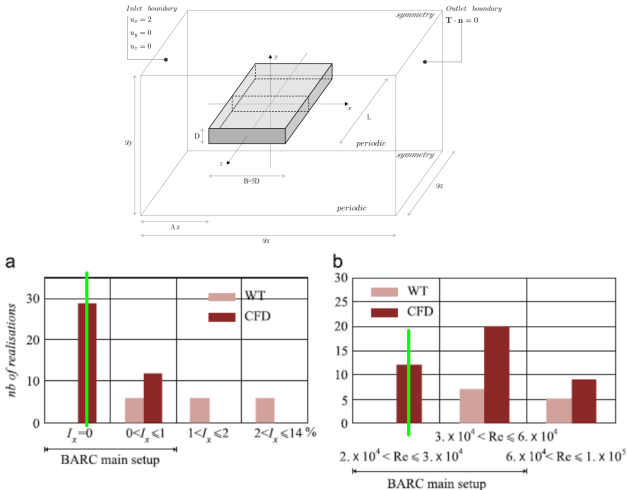
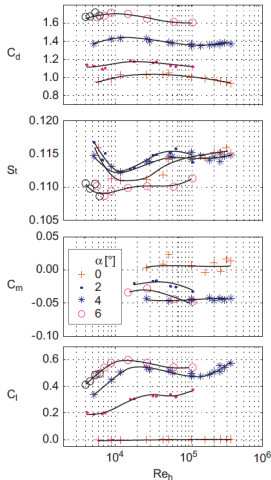


Figure: Comparisons with other simulations [4].

Reynolds dependence



The adopted Re is equal to 2.1×10^4 . In the case of the 5:1 rectangular cylinder only a weak dependence is found in the range from $Re = 2.0 \times 10^4 - 1.0 \times 10^5$.

Figure: Re dependence for the rectangular cylinder 5:1 at different attack angles [5].

LES turbulence modeling

LES filtered equations

$$\frac{\partial \overline{u}_i}{\partial x_i} = 0 \quad (1)$$

$$\frac{\partial \overline{u}_i}{\partial t} + \frac{\partial \overline{u}_i \cdot \overline{u}_j}{\partial x_j} = -\frac{1}{\rho} \frac{\partial \overline{p}}{\partial x_i} + \frac{\partial \overline{\tau}_{ij}}{\partial x_j} - \frac{\partial \tau_{ij}^s}{\partial x_j} \quad (2)$$

$$\overline{\tau}_{ij} = 2\mu \left[\frac{1}{2} \left(\frac{\partial \overline{u}_i}{\partial x_j} + \frac{\partial \overline{u}_j}{\partial x_i} \right) - \frac{1}{3} \frac{\partial \overline{u}_k}{\partial x_k} \delta_{ij} \right] \quad (3)$$

Smagorinsky-Lilly model

$$\tau_{ij}^s = \nu_t \left(\frac{\partial \overline{u}_i}{\partial x_j} + \frac{\partial \overline{u}_j}{\partial x_i} \right) \quad (4)$$

$$\nu_t = (C_s \Delta_g)^2 (2 \overline{\mathbf{S}}_{ij} \cdot \overline{\mathbf{S}}_{ij})^{\frac{1}{2}} \quad (5)$$

Finite Volumes Numerical Schemes adopted for LES

Analysis setup

- Pressure-velocity coupling is obtained by using the PIMPLE algorithm;
- the time integration is performed with the two-step implicit second-order Backward scheme;
- centered second-order differentiation scheme is adopted for diffusive terms;
- the Linear Upwind Stabilized Transport (LUST) scheme is adopted for the advective term;
- the adopted non-dimensional time step (based on D) is $\Delta t^* = 5.0e - 3$;
- the maximum *Courant* number obtained is $Co = 2.4$;

RANS

RANS setup

- the RANS simulations are run in a **2D framework**;
- the adopted turbulence model is the $k - \omega$ *sst*;
- Second-order accurate upwind schemes are adopted for all terms in the model equations;
- Boundary conditions are the same adopted for the LES simulations but periodic conditions are replaced with symmetry.
- the adopted non-dimensional time step (based on D) is $\Delta t^* = 1.0e - 2$;
- the maximum *Courant* number obtained is $Co = 4.6$;
- the maximum y^+ obtained is equal to 2.4, therefore the first cell is in the viscous sub-layer.

CINECA & OpenFOAM

- All the simulations have been performed by using the open source **Finite Volume software OpenFOAM** .
- A preliminary scalability test suggest to run cases on **120 CPUs**.
- All the analysis are performed at the **CINECA PLX cluster**.

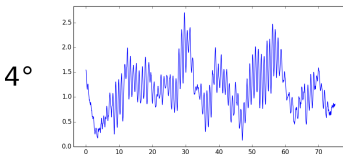
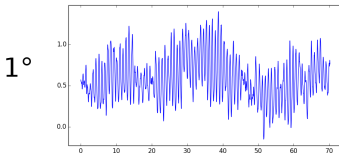
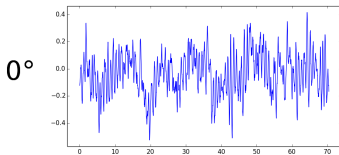
Open▽FOAM



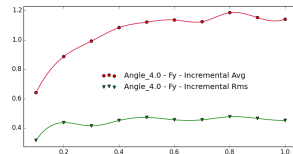
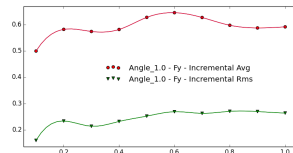
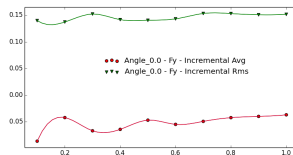
Initialization and Analysis Time

- The flow is initialized with a Laplacian;
- Simulations are run over a total time of 800 non-dimensional time units;
- Only the last 500 are considered in the post processing of data in order to avoid the effects of the flow initialization.

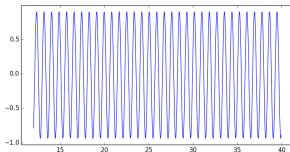
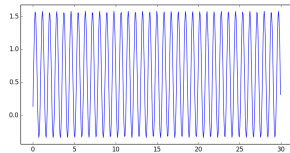
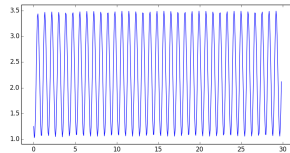
Lift Signal



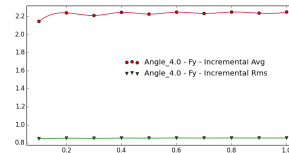
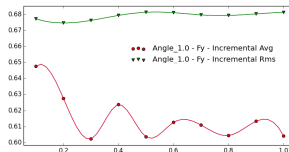
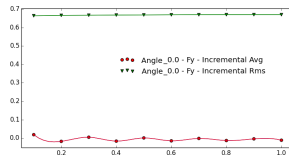
Lift Statistics



Lift Signal

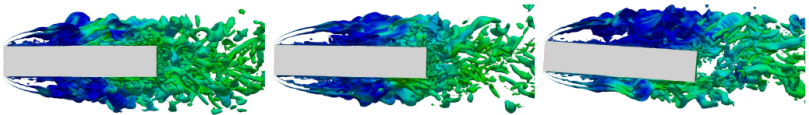
 0°  1°  4° 

Lift Statistics



Flow Topology

LES simulations

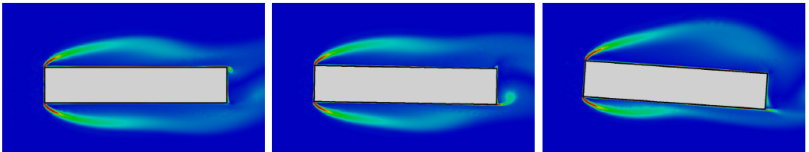


0° degrees

1° degree

4° degrees

RANS simulations



0° degrees

1° degree

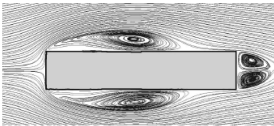
4° degrees

RANS suppresses the shear layer instabilities and replace it with a smooth shear layer, due to high turbulent viscosity.

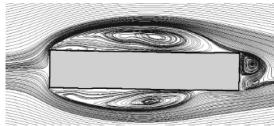
Vorticity

Averaged Streamlines

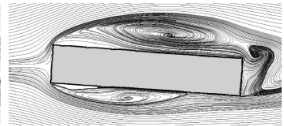
LES simulations



0° degrees

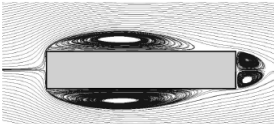


1° degree

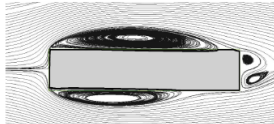


4° degrees

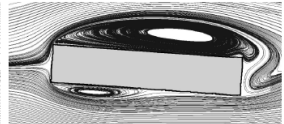
RANS simulations



0° degrees



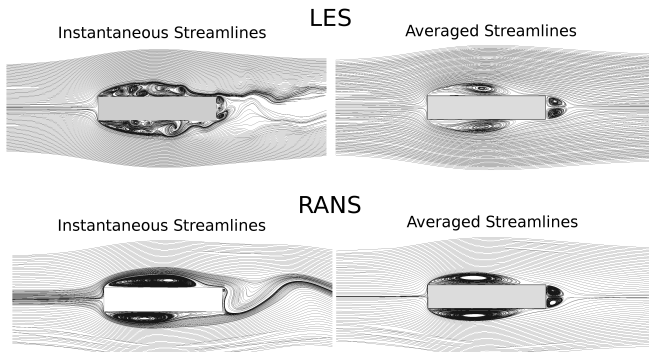
1° degree



4° degrees

Averaged Streamlines

- The two models provide reattachment length in good agreement for 0° and 1° .
- The RANS model presents an elliptical bubble, while the LES predicts an elongated drop shape. This difference is mainly due to the vortex organization inside the bubble.



Bulk Parameters

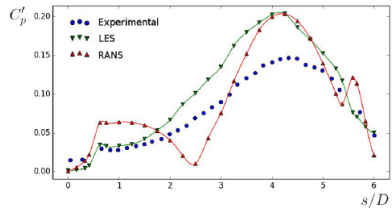
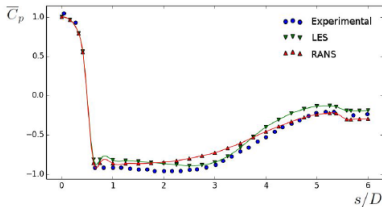
- At 0° both models are in good agreement with experimental data;
- When the attack angle increases the differences between numerical results and experimental data increases;
- At 4° the RANS model highlights a change of the flow topology and overestimates the lift coefficients, while the LES model show a smoother transition, underestimating it.

Angle	Source	C_D	C'_D	C_L	C'_L	St
0°	LES	1.02	0.020	-0.05	0.19	0.132
	RANS	1.12	0.018	-0.02	0.81	0.121
	Pigolotti et al. (2015)	1.13	-	-0.04	-	0.118
	Schewe (2013)	1.00	-	0.00	-	0.112
	Bruno et al. (2011)	0.96 to 1.03	-	-0.315 to -0.0024	0.2 to 0.73	0.112 to 0.122
	Grozescu (2011)	0.97 to 0.98	-	-0.097 to 0.0043	0.52 to 0.65	0.107 to 0.111
	Mannini (2011)	0.97 to 1.07	-	0.0032 to 0.047	0.42 to 1.07	0.094 to 0.102
1°	LES	1.05	0.031	0.74	0.33	0.119
	RANS	1.16	0.056	0.75	0.85	0.116
	Pigolotti et al. (2015)	1.28	-	0.96	-	0.120
4°	LES	1.26	0.056	1.44	0.57	0.116
	RANS	1.57	0.158	2.80	1.06	0.117
	Pigolotti et al. (2015)	1.63	-	2.02	-	0.126
	Schewe (2013)	1.40	-	2.55	-	0.115

Central Section Statistics

 0°

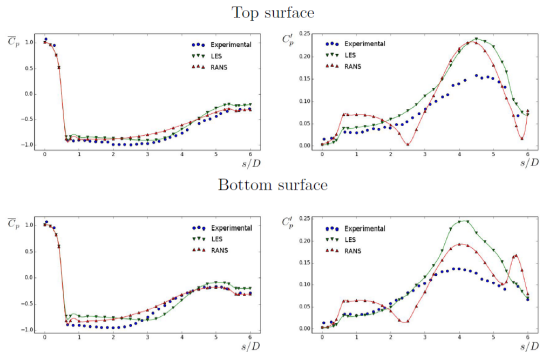
- At 0° both models are in good agreement with experimental data in terms of time-averaged $\overline{C_p}$;
- Also the rms of C_p obtained from the two simulations is in good agreement with the experimental one, even if the numerical solution overestimates the peak of C_p' of about 30%.
- The RANS model shows a minimum of C_p' not observed experimentally.



Central Section Statistics

1°

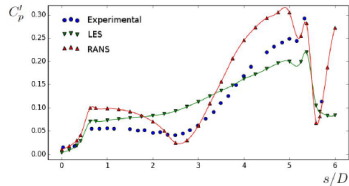
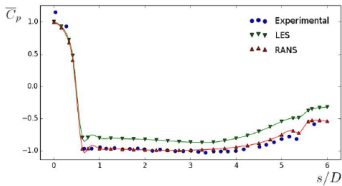
- At non-null attack angles differences within models and experimental results increase;
- At 1° main differences are recorded at the bottom surface, where LES predicts a sharper pressure recovery;
- RANS model predicts a simplified separation bubble topology, so as an outcome, the pressure recovery appears to be very smooth;



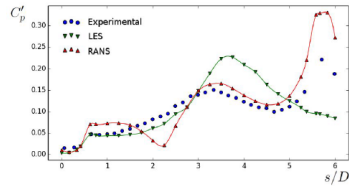
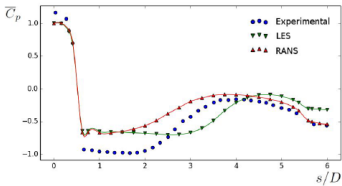
Central Section Statistics

4°

Top surface

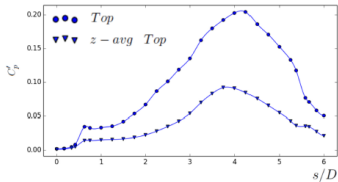


Bottom surface

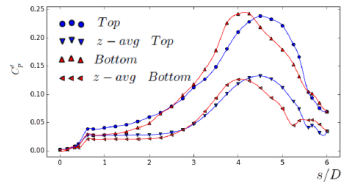


- At 4° the two numerical approach differ significantly, as highlighted by bulk parameters;
- The mean C_p on the top side is well represented by RANS and LES, even if the latter shows an almost constant offset;
- RANS predicts a reattachment of the vortex on the top side, while LES does not;
- At the bottom surface the trend observed at 1° is confirmed.

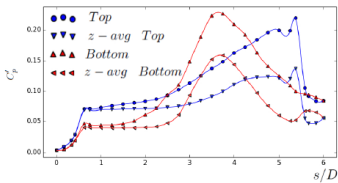
Z-averaged Statistics



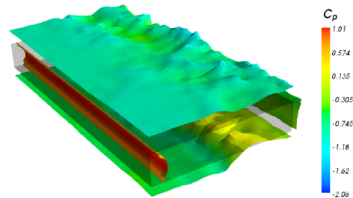
(a)



(b)



(c)



(d)

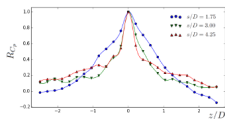
Figure: z-averaged statistics: 0° (a), 1° (b), 4° (c) and instantaneous C_p at 4° (d)

Z-averaged Statistics

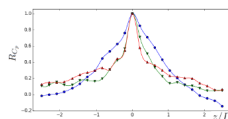
- At 0° the z-averaged C'_p is almost 50% of the not averaged value in all points, indicating that the correlation length is almost constant;
- At 1° and 4° the reduction is lower and increases towards the trailing edge, indicating that the flow three-dimensionality is higher in that region.
- No remarkable differences are observed in the peaks position since they are mainly due to two-dimensional mechanisms.

Spanwise Averaged Statistics and Correlations

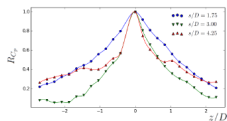
Z-correlations



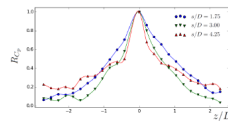
0° Top



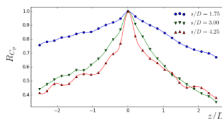
0° Bottom



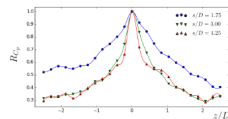
1° Top



1° Bottom



4° Top



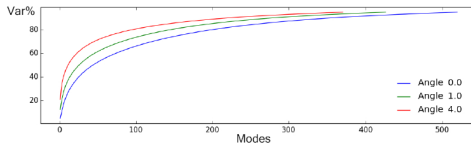
4° Bottom

Z-correlations

- When the attack angle increases, the along span correlation increases, especially on the top surface, therefore the two-dimensionality of the flow is increased.
- At 4° correlations remain high along the span, indicating that the adopted domain is too small in this case. If correlations do not go to approximately zero, periodic boundary conditions affect results.

CPT : Rate of Convergence

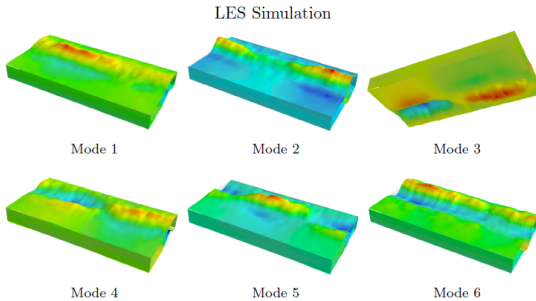
- The number of modes needed to reach the 95% of the variance strongly depends on the attack angle;
- At 4° the recovery of the variance is quicker than at 0° and 1°;



Mode	0 degrees		1 degree		4 degrees	
	LES [%]	RANS [%]	LES [%]	RANS [%]	LES [%]	RANS [%]
1	4	77	12	77	20	80
2	3	21	5	21	8	19
3	3	1	3	1	5	-
4	2	-	2	-	3	-
5	2	-	2	-	2	-
6	2	-	2	-	2	-

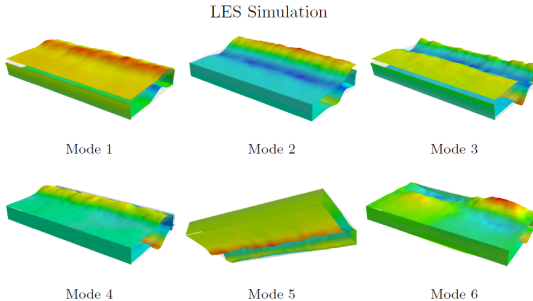
CPT LES: 0°

- At 0° the flow three-dimensionality is clear since the Mode 1.



CPT LES: 4°

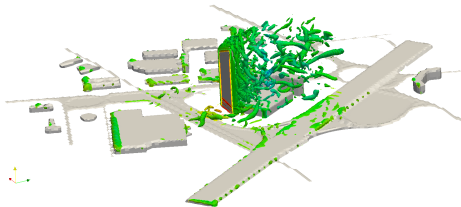
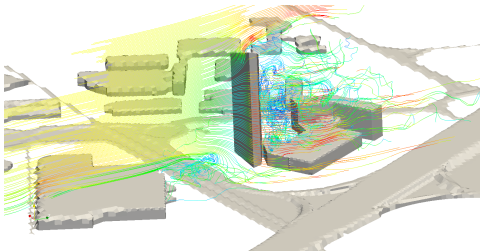
- At 4° the flow two-dimensionality is increased, being the first marked three-dimensional mode the Mode 6.



Summary

- Differences observed between RANS and LES at non-null attack angles highlights the high sensitivity of the flow with respect to the turbulence model;
- The flow two-dimensionality increases at non-null attack angles concentrating energy in the first CPT modes. Such result indicates that a larger computational domain is required when non-null attack angles are considered.

Not only benchmarks.....



Not only benchmarks.....

Some Quotes

"The judicial presumption of innocence does not hold in CFD. CFD results are wrong, until proven otherwise."

Blocken, 2014.

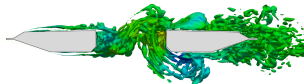
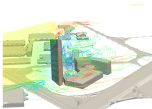
"Good mental health in a fluid or CFD modeler is always indicated by the presence of a suspicious nature, cynicism and a 'show me' attitude. These are not the best traits for a life mate or a best friend, but they are essential if the integrity of the modeling process is to be maintained."

Meroney, 2004.







ALMA MATER STUDIORUM
UNIVERSITÀ DI BOLOGNA

Mattia Ricci
mattia.ricci10@unibo.it



DICAM-Laboratory of Computational Mechanics

-  de Miranda, S., Patruno, L., Ricci, M., Ubertini, F., 2015.
Numerical study of a twin box bridge deck by using RANS and LES approaches.
Engineering Structures, Under Review.
-  Braun, A. L., Awruch, A. M., 2009.
Aerodynamic and aeroelastic analyses on the CAARC standard tall building model using numerical simulation.
Computers and Structures, **Vol 87**, page 564-581 (2009).
-  Janssen, W.D., Blocken, B., van Hooff, T., 2013.
Pedestrian wind comfort around buildings: Comparison of wind comfort criteria based on whole-flow field data for a complex case study.
Building and Environment, **Vol 59**, page 547-562 (2013).
-  Bruno, L., Salvetti, M. V., Ricciardelli, F., 2014
Benchmark on the Aerodynamics of a Rectangular 5:1 Cylinder: An overview after the first four years of activity.

Journal of Wind Engineering and Industrial Aerodynamics,
Vol 126, page 87-106 (2014).



Schewe, G., 2013

Reynolds-number-effects in flow around a rectangular
cylinder with aspect 1:5

Journal of Fluids and Structures, **Vol 39**, page 15-26
(2013).